Double cobalt-catalyzed atroposelective C–H activation: One-step synthesis of atropisomeric indoles bearing vicinal C–C and C–N diaxes

Amandine Luc, João C.A. Oliveira, Philipp Boos, Nicolas Jacob, Lutz Ackermann, Joanna Wencel-Delord

Double Cobalt-Catalysed Atroposelective C-H Activation: One-step Synthesis of Atropisomeric Indoles bearing Vicinal C-C and C-N Diaxes

Amandine Luc,[a] João C. A. Oliveira,[b,c] Philipp Boos,[b,c] Nicolas Jacob,[a] Lutz Ackermann*,[b,c]

Joanna Wencel-Delord*[a]

[a]*Laboratoire d'Innovation Moléculaire et Applications (LIMA – UMR CNRS 7042) Université de Strasbourg/Université de Haute Alsace SynCat-H, ECPM, 25 Rue Becquerel, 67087 Strasbourg, France*
[b]*Institut für Organische und Biomolekulare Chemie Georg-August-Universität Göttingen, Tammannstr. 2, 37077 Göttingen, Germany*
[c]*Wölher Research Institute for Sustainable Chemistry, Georg-August-Universität, Tammannstr. 2, 37077 Göttingen, Germany*

ABSTRACT: Expanding the borders of asymmetric synthesis by designing original chiral molecules and sustainable strategies to synthesize them holds great promise not only for the pharmaceutical industry but also for material science and agrochemistry. In particular, straightforward, one-step synthesis of enantiopure scaffolds featuring two proximal chiral axes presents a great scientific challenge. Herein, unique asymmetric C-H activation reaction has been used to achieve the first intermolecular direct arylation-type reaction, affording indoles bearing simultaneously C2-atropisomeric Ar-Ar' axis together with C-N axial chirality. Remarkably, the desired reactivity could be achieved using a chiral cobalt complex as a sustainable and cheap catalyst, thus delivering the expected multiatropisomeric compounds in high yields and excellent diastereoselectivities and enantioselectivities. In addition, detailed mechanistic studies provide fundamental comprehension of this unique transformation.

Introduction

Chirality, the unique feature of nature, has been continuously inspiring modern research and attracting the attention of the scientific community. Initially considered rather as a scientific curiosity and fundamental research challenge, implementation of stereogenic information and escaping from flat-land while designing complex molecules for biological purposes,[1] agrochemicals[2] and advanced organic material,[3] is now a widely recognized tool to meet superior properties. While chirality has been, for decades, mainly attributed to a presence of a

C-stereogenic center, other chiral elements such as planar-chirality, heteroatom-centered point-chirality, atropoisomerism or axial C-N axis have progressively established themselves as valuable and intriguing stereogenic motifs, thus providing additional opportunities for the design of enantiopure molecules of interest (Figure 1a). Recently, in order to further enhance the benefits arising from a stereogenic character of a molecule, assembling compounds bearing multiple proximal stereoelements has emerged as an innovative research axis (Figure 1b).[4] While a diversity of synthetic approaches, including olefins' functionalization and stereoselective aldol reactions, can be envisioned to access in one step molecules bearing two proximal stereocenters, conception of strategies delivering vicinal multi-atropisomeric compounds is infinitely more challenging. Recently, a few ingenious approaches have been designed to assemble in one step complex chiral molecules bearing contiguous atropo-biaryl axes. In particular cycloaddition-type reactions,[5] organocatalyzed [3+3] or [3+2] annulations,[6] intramolecular aldol condensations[7] or central-to-axial chirality transfer[8] reactions proved their potential.

In clear contrast, the synthesis of chiral scaffolds featuring proximal atropisomeric Ar-Ar' and N-Ar axes is considerably more challenging and remains an almost uncharted research field. The difficulty arises from frequently relatively low atropostability of the Ar-N bond combined with the limited synthetic approaches providing a stereoselective synthesis of C-N atropisomeric compounds.[9] In consequence, one-step synthesis of such compounds remains extremely rare and mainly limited to Rh-catalyzed [2+2+2] cycloaddition,[10] oganocatalyzed intramolecular heteroaromatic ring formation[11] or very recent intramolecular annulation-type protocol (Figure 1d).[12] Therefore, while considering the expanding interest in such products as illustrated by modern drug-design (such as BMS-986142,[13] an inhibitor of BTK and Sotorasib[14] for example, Figure 1c),[15] design of innovative synthetic routes furnishing chiral molecules bearing both biaryl and Ar-N axial axes is urgently needed.

The last decade was clearly marked by major advances achieved in the field of C-H activation.[16] This methodology, considered as scientific curiosity twenty years ago, is nowadays a well-established tool to assemble molecular complexity in a sustainable manner, using simple starting materials and limiting waste generation. Consequently, implementation of a chirality transfer within direct functionalization reactions has been gaining growing importance, resulting in the appearance of original and complex enantiopure molecules, difficult to access via standard asymmetric synthesis routes.[17] Progressively, the asymmetric C-H activation mindset inspired the design of conceptually unprecedented transformations, delivering in one-step multi-chiral scaffolds, bearing for example axial and point chirality[18] or two atropisomeric axes.[19] However, the majority of these transformations thus far required the use of expensive and rare transition metal-based complexes, including chiral palladium- and rhodium-catalysts. In clear contrast, the exploitation of more sustainable, less expensive, and abundant 3d-metal chiral catalysts[20] to promote asymmetric C-H activation reactions is still limited.[21] While considering the importance of multi-atropisomeric scaffolds featuring N-Ar bond, combined with the lack of synthetic routes to prepare them and the potential of asymmetric C-H activation to pave the way towards conceptually innovative synthetic disconnections, implementation of the C-H activation mindset to assemble such compounds thus present a formidable scientific challenge.

Following this goal, we report herein a unique protocol furnishing complex chiral molecules featuring both Ar-Ar' and N-Ar axes. The salient features of this reaction is: 1) the utilization of simple indole precursors, 2) high reactivity and excellent diastereo- and enantio-selectivities achieved while using low-valent cobalt-catalyst, 3) mild reaction conditions, and 4) the possibility to prepare unprecedented biatropisomeric indoles (Figure 1e).

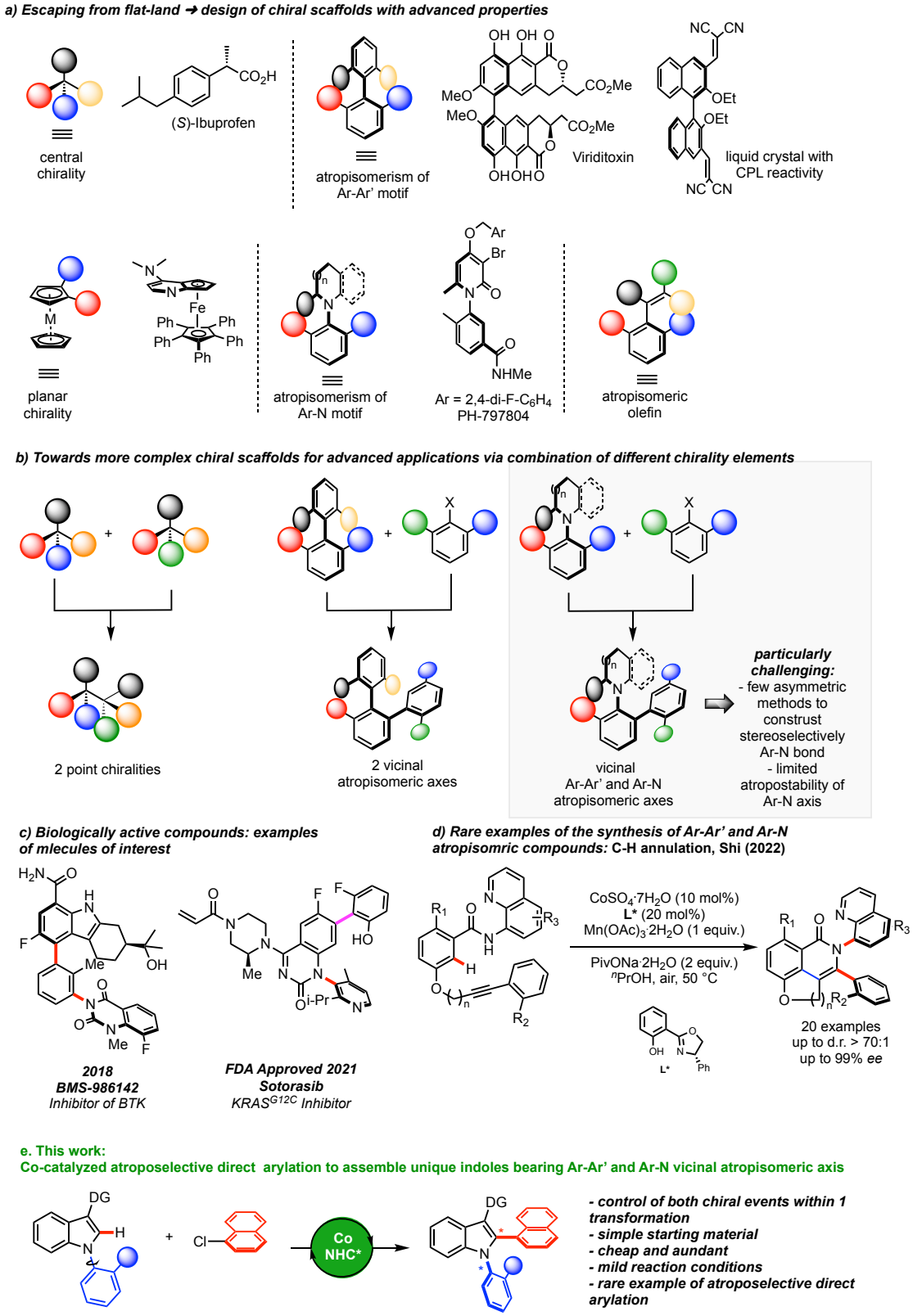

Figure 1 : From simple chirality to innovative tridimensional structures for advanced applications. a) examples of different types of chirality and their applications; b) recent advances: design and synthesis of multichiral molecules with chirality elements in close proximity; c) recent design of biologically active scaffolds bearing both C-C and C-N chiral axes; d) example of simultaneous generation of C-C and C-N atropisomeric axes via intramolecular reaction; e) application of Co-catalyzed asymmetric C-H arylation to assembly unique indoles with C-C and C-N chiral axes.

I. Optimization of the reaction

While conceiving the herein targeted double atroposelective C-H activation, we hypothesized that *N*-arylated indoles bearing a directing group at C3 positions should react efficiently under the C-H activation protocol (**Erreur ! Source du renvoi introuvable.**).[22] Installation of an additional substituent at the C2 position should potentially induce not only the newly generated C2-Ar bond but also prevent the rotation of the Ar-N motif thus delivering the desired indole product with two perfectly controlled chiral axes. Following this hypothesis, *N*-aryl-indole **1a** was selected as a standard substrate, together with 1-chloronaphtalene **2**. An unusual *meta*-substituted NHC-ligand **L1**[23] gave promising results as the desired product could be isolated in 70% yield as 87:13 mixture of two diastereoisomers and an excellent 95:5 enantiomeric ratio for the major one. Interestingly, detailed ligand design revealed that the presence of finely adjusted substituents at *ortho*-, *meta*- and *para*-positions is crucial, as in the presence of **L3**, **L5,** and **L7** either enantioselectivity or diastereoselectivity could not be reached. Non-*meta*-substituted ligand **L3**, delivered both diastereomers of the products as racemates (entry 3), thus clearly indicating the pivotal role of this substituent in the chiral induction. In contrast, both *ortho*- and *para*-substituents are crucial to enhance catalytic activity and diastereoselectivity. In addition, the optimization of the reaction conditions confirmed the best reactivity in THF solvent and also the importance of 1:2 metal to ligand ratio. Remarkably, this transformation is specific to cobalt-catalysis as no reaction occurred while using various other standard Pd, Ru, Mn, Ni, and Fe catalysts (entry 13). Test reactions confirmed that in the absence of cobalt, or the ligand, no reaction occurred, while chloronaphthalene clearly outcompeted other naphthalene coupling partners (entries 10-11). Finally, a reduced reaction time translated into a further improvement of the chirality transfer (entry 12).

Table 1: Optimization of the reaction conditions of atroposelective direct Co-catalyzed arylation

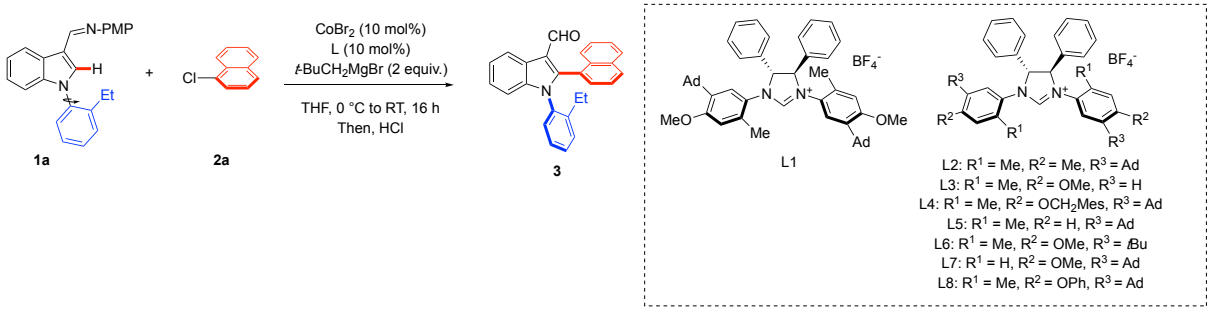

Entry	***Ligand or cat.***	***d.r.***	***yield %***	***er major dia***	***er minor dia***
1	L*1	87 : 13	70%	95 : 5	61 : 39
2	L*2	68 : 32	50%	95.5 : 4.5	55 : 45
3	L*3	30 : 70	33 %	50 :50	50 :50
4	L*4	66 : 34	43%	96 : 4	50:50
5	L*5	50 : 50	ND	ND	ND
6	L*6	78 : 22	35%	96.5 : 3.5	56.6 : 43.5
7	L*7	50 : 50	ND	ND	ND
8	L*8	67 : 33	38%	90 : 10	52 : 48
9	L1[a]	97 : 03	80	96.5 : 3.5	ND
10	1-Bromonaphtalene instead of 1-chloronaphtalene[a,c]	72 :28	20	56.5:43.5	50 :50
11	1-Iodonaphtalene instead of 1-chloronaphtalene[a,c]	50 :50	Traces	ND	ND
12	**L1[a,b]**	**97 :03**	**80**	**96:04**	**ND**
13	$PdCl_2$, $Pd(OAc)_2$, $[Ru(p\text{-cymene})Cl_2]_2$, $RuCl_3$, $MnBr_2$, $NiCl_2$, $Fe(acac)_3$[a,c]	NR	-	-	-

Reaction conditions: **1a** (0.1 mmol scale, 1 equiv.), **2** (0.2 mmol scale, 2 equiv.), THF (0.286 M). [a]20 mol% of ligand; [b]7h reaction time; [c]with L*1. Reported yields are isolated yields. The diastereomeric ratio (d.r.) was determined by ^{1}H NMR spectroscopy. The enantiomeric ratio (*er*) was determined by chiral HPLC.

II. Scope of the reaction

With the optimized conditions in hand, the scope of this reaction was evaluated. First, the impact of the electronic and steric properties of the Ar-substituent of the N-atom of indole was investigated (**Scheme 1**). Indeed, the steric hindrance at the *ortho*-position of this aromatic ring controls the atropostability of the newly induced C-N axis. Me-, Et-, and Ph-*ortho*-substituents

performed equally well, delivering the desired products **3a** – **3c** in high enantioselectivity, diastereoselectivity, and yields. In clear contrast, further increased steric hindrance around the C-N bond (*i*-Pr group) resulted in lower reaction efficiency and diastereoselectivity, arguably due to the restricted rotation around the C-N of the corresponding substrate. Naphthyl-substituted indole **1e** performed well, delivering the desired product in good yield and diastereoselectivity, but the loss of the enantioselectivity was observed. In contrast, the reaction tolerates *ortho*-OCF_3 substituent, affording **3f** in 65% yield and with good control of the stereoselectivity.

Subsequently, the scope of the indole core was investigated. Various electron donating, as well as electron withdrawing groups (fluorine or trifluoromethyle for example), were well tolerated regardless of their position on the indole substrate, thus furnishing the arylated products in moderate to good yields and with high control of both, diastereoselectivity and enantioselectivity. Generally considered as challenging, the thioether motif, turned out to be perfectly compatible with this asymmetric transformation, as the product **3l** was isolated in 83% yield and excellent chiral induction (er of 99:1). Remarkably, azaindole **3s**, a potential drug candidate, was delivered in 80% yield, 95:5 d.r and 96.5:3.5 e.r. thus clearly illustrating the potential of this protocol for drug design.

Finally, the scope of naphthyl-coupling partners was evaluated. Despite the increased steric hindrance, chloro-pyrene was found to be an efficient coupling partner in this reaction, providing **3u** in good yield and high stereoselectivities. *Para*-substituted chloro-naphthyls showed good reactivity under the standard reaction conditions, furnishing efficiently **3v**, **3w**, and **3x**. Finally, the compound **3z** was obtained in 25% yield but with an excellent control of the diastereoselectivity but with loss of enantioselectivity.

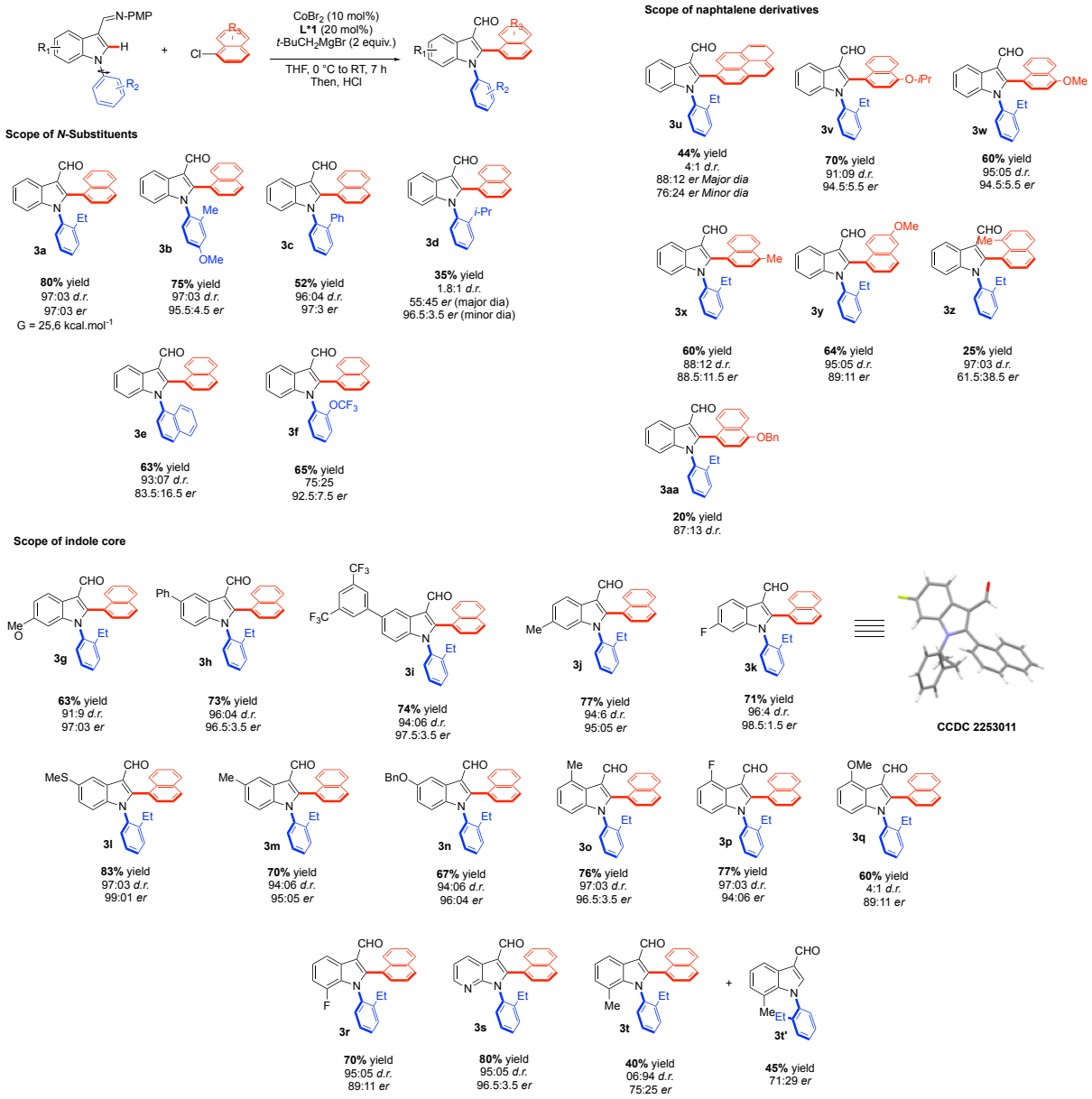

Scheme 1 : Scope of the reaction. *(The scope was performed on a 0.2 mmol scale. Reported yields are isolated yields. The diastereomeric ratio (d.r.) was determined by ^{1}H NMR spectroscopy. The enantiomeric excess (ee) was determined by chiral HPLC.)*

The absolute a$R_{C\text{-}N}$,a$S_{C\text{-}C}$ configuration of the obtained compounds was unambiguously confirmed based on the X-ray structure of **3k**.[24] In addition, the experimental study of the epimerization of **3a** revealed the rotational barrier of the C-C axis of $\mathbf{\Delta G^1_{C\text{-}C}}$ = 25.6 kcal mol^{-1}, while the value of the rotational barrier of the C-N axis could not be reached experimentally even after a prolonged heating at 80 °C. These experimental results thus indicate a surprisingly strong atropostability of the C-N motif. Accordingly, the measurements of the rotational barrier

of C-C axis at 80 °C with chiral HPLC clearly shows equilibrium between two diastereomers reached after several hours while both diastereomers remains enantiomerically enriched.

III. Gram-scale synthesis and and Post-functionalization

To further illustrate the synthetic value of this newly developed transformation, a gram scale reaction was performed (Scheme 2), yielding **3a** in high 72% yield and with no impact on the diastereoselectivity (*d.r.* 96:04) and enantioselectivity (91% *ee*). Moreover, washing with cold diethyl ether afforded the product (61% yield) as a single diastereoisomer.

Subsequent post-functionalizations revealed that the aldehyde motif present at C3-position can be astutely used to direct a direct amination into the C4-position[25,26] delivering the highly decorated indole **4a** in good yield, while conserving its stereochemical purity. The cleavage of the Ts group performed well, delivering **4b** in 76% yield and same *d.r.* and *e.r.* Alternatively, a ketone-derived product **4c** was accessed easily and under mild conditions. with high diastereo- and enantioselectivity,

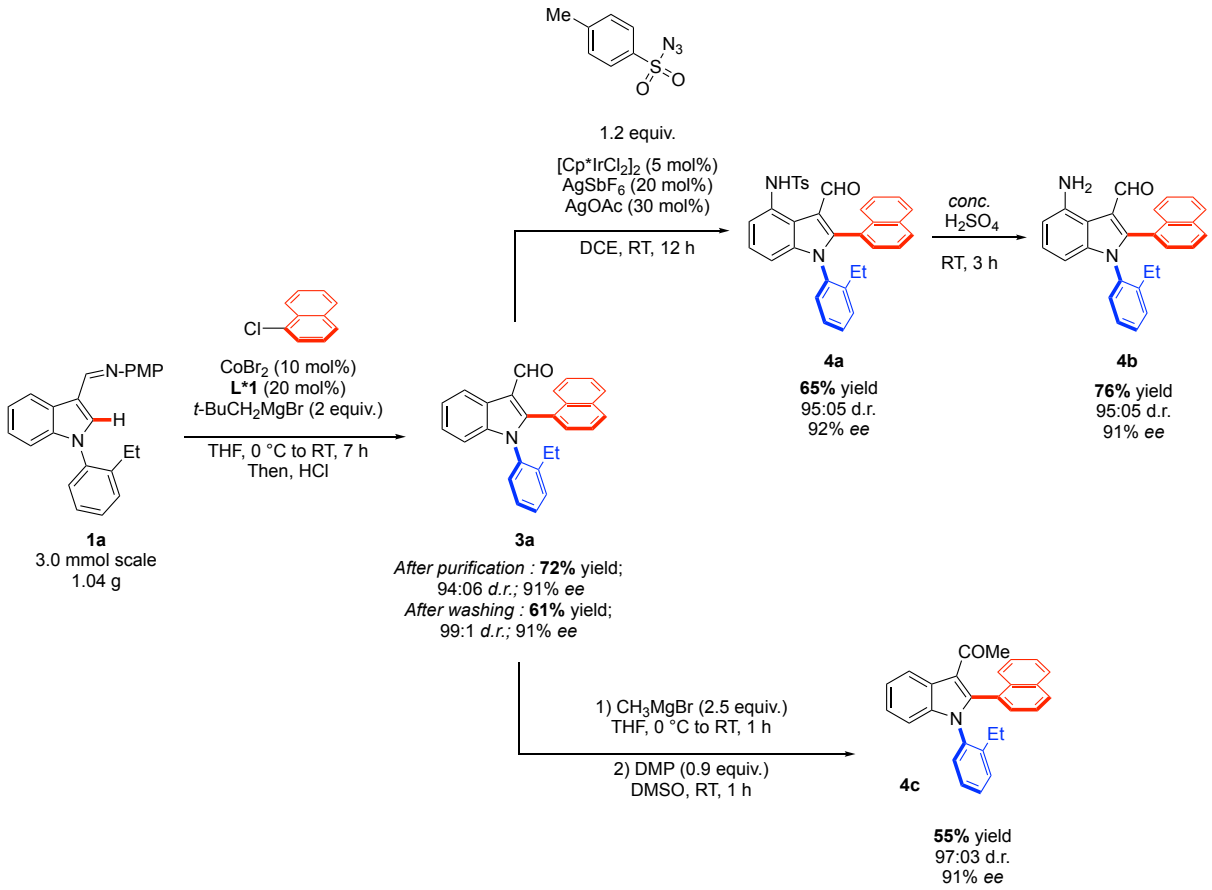

Scheme 2 : Large-scale synthesis and post-modifications.

IV. Mechanistic studies

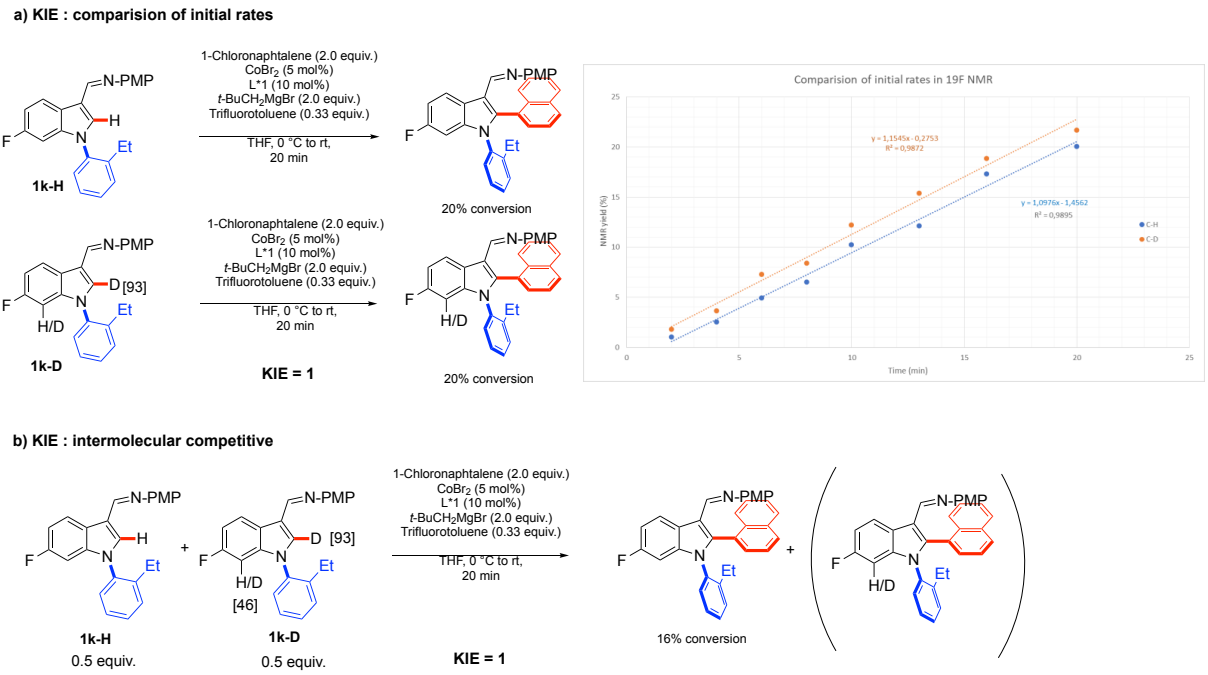

Scheme 3 : Investigations of the KIE.

In order to shed light on the mechanism of this transformation, combined experimental and theoretical mechanistic investigations were undertaken (Scheme 3). The kinetic isotope effect was measured via both, parallel initial rate comparison and competition experiments, indicating in both cases value close to 1. Therefore, the C-H activation is expected to be non-rate-determining. Besides, the linear correlation between the optical purity of the ligand used and the enantiomeric excess of the product formed clearly were suggestive of the absence of the non-linear effect and thus indicated implication of monomeric Co-L species (See SI Figure 5).

Intrigued by the origins of the enantioselectivity and diastereoselectivity, these were interrogated by computational mechanistic studies through DFT calculations at the ωB97XD/def2-TZVPP+SMD(THF)//TPSS-D3(BJ)/def2-SVP level of theory for C–H activation, oxidative addition and reductive elimination elementary steps (Figure 2).[25] Given the intrinsic nature of the cobalt(I) intermediates **I-1**, both high-spin (triplet) and low-spin (singlet) complexes were taken into consideration for the C–H activation as well as for the oxidative addition elementary steps (See SI Figures 6-10). The latter gives origin to cobalt(III) complexes **I-3**, which lead to C–C bond formation through reductive elimination [**TS(4-5)**]. Given the d^6 electronic configuration of the cobalt(III) all possible spin states were assessed, namely high-spin (quintet), low-spin (singlet) and an intermediate-spin (triplet) (See SI Figures 6-10). The triplet energy surface revealed to be the energetically preferred pathway over all the considered spin states with the absence of a spin-crossover reactivity. An assessment of the energy profile for the experimentally observed a$R_{C\text{-}N}$,a$S_{C\text{-}C}$-enantiomer shown that C–H activation proceeds through a facile ligand-to-ligand hydrogen transfer (LLHT) [**TS(1-2)**] with a barrier of 9.5 kcal mol^{-1}. The oxidative addition revealed to be the rate determining step, presenting an energy barrier hight of 11 kcal mol^{-1} [**TS(3-4)**], whereas for reductive elimination a barrier of 3.2 kcal mol^{-1} was calculated [**TS(4-5)**] (Figure 2). The oxidative addition for the a$R_{C\text{-}N}$,a$S_{C\text{-}C}$-enantiomer revealed to be stabilized by 2.4 kcal mol^{-1} over the a$S_{C\text{-}N}$,a$R_{C\text{-}C}$-enantiomer (Figure 2). This energy difference can be translated into an enantiomeric excess of 98% which is in good agreement with the experiments. The stabilization of the a$R_{C\text{-}N}$,a$S_{C\text{-}C}$ -enantiomer over the a$S_{C\text{-}N}$,a$R_{C\text{-}C}$-enantiomer may result from weak attractive dispersion interactions from the naphthyl and the N-alkylphenyl moiety of the substrate in the transition state **TS(1-2)**, which is absent in the a$S_{C\text{-}N}$,a$R_{C\text{-}C}$-enantiomer (Figures 3 and 4). Additionally, calculations in the absence of dispersion corrections resulted in a change in the

enantioselectivity, highlighting the importance of dispersion forces in such systems. Intrigued by the diastereoselectivity origins, and if this would be dictated before the rate determining step, the oxidative addition of the 1-chloronaphthalene, attention was given to the rotation barrier over the C–N axis in the cyclometalated complex **I-2** for the experimentally preferred a$R_{C\text{-}N}$,a$S_{C\text{-}C}$ -enantiomer. This was calculated to be 27.6 kcal mol^{-1} which corresponds to a half-time ($t_{1/2}$) of 221 days. Such indicates that the C–H activation elementary step highly influences the diasterioselectivity.

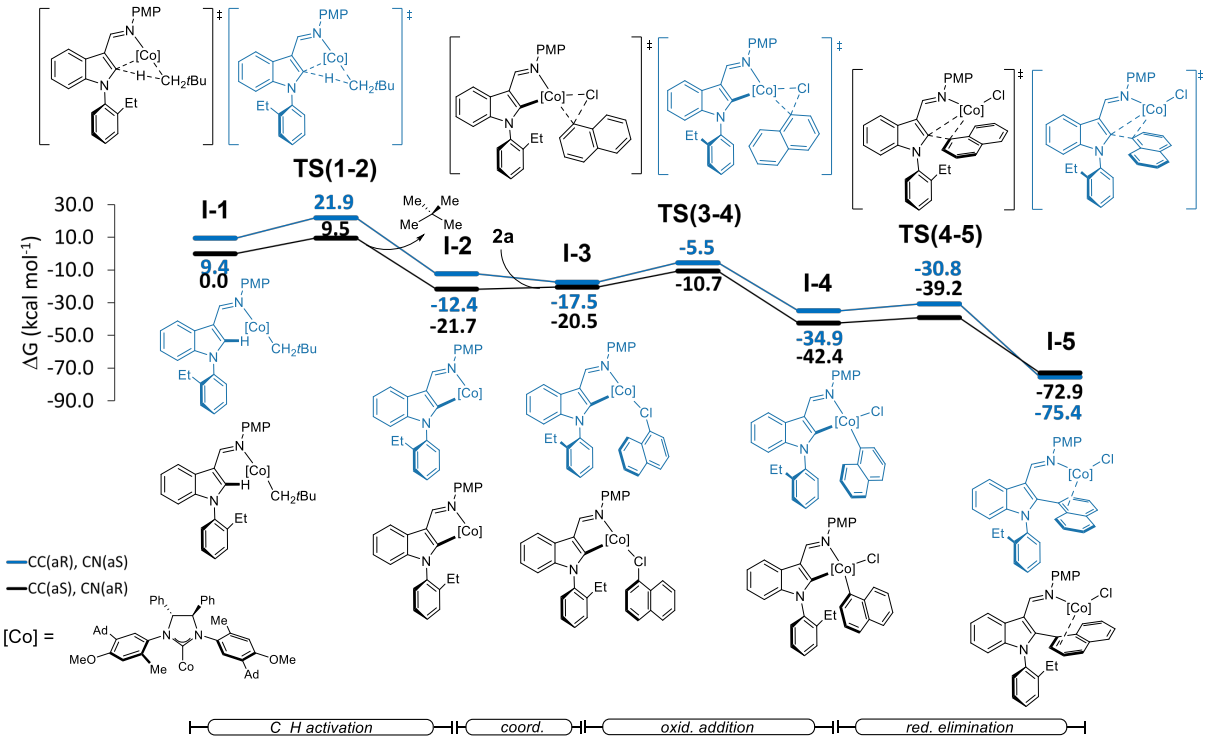

*Figure 2 : Computed relative Gibbs free energies ($\Delta G_{298.15}$) in kcal mol^{-1} for the oxidative addition and reductive elimination elementary steps, in the most stable triplet surface, for the a$S_{C\text{-}N}$,a$R_{C\text{-}C}$- and a$R_{C\text{-}N}$,a$S_{C\text{-}C}$-enantiomers at the ωB97XD/def2-TZVPP+SMD(THF)//TPSS-D3(BJ)/def2-SVP level of theory with the chiral ligand **L*1**.*

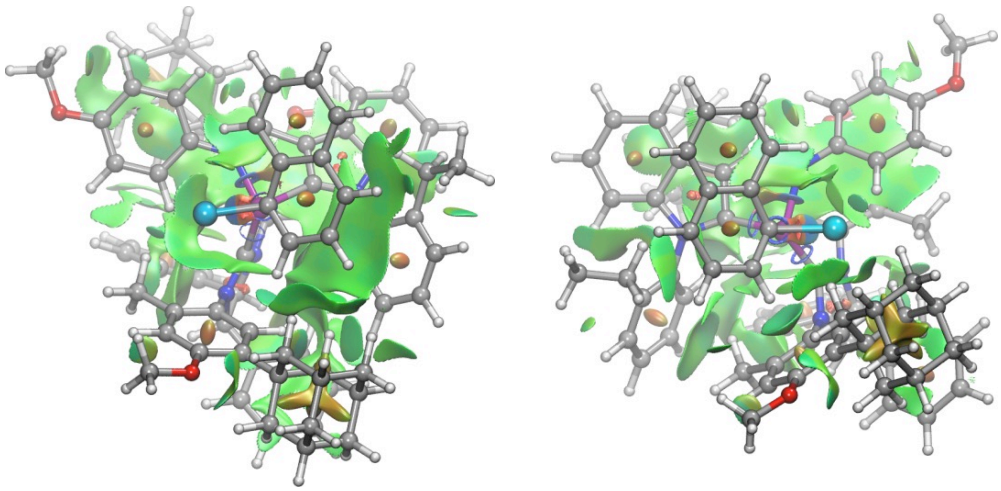

Figure 3 : Visualization of the non-covalent interactions calculated with the help of the NCIPLOT program for the transition states involved in the oxidative addition step for both $aS_{C\text{-}N},aR_{C\text{-}}$ - and $aR_{C\text{-}N},aS_{C\text{-}C}$ -enantiomers. In the plotted surfaces, red correspond to strong repulsive interactions, while green and blue correspond to weak and strong interactions, respectively.

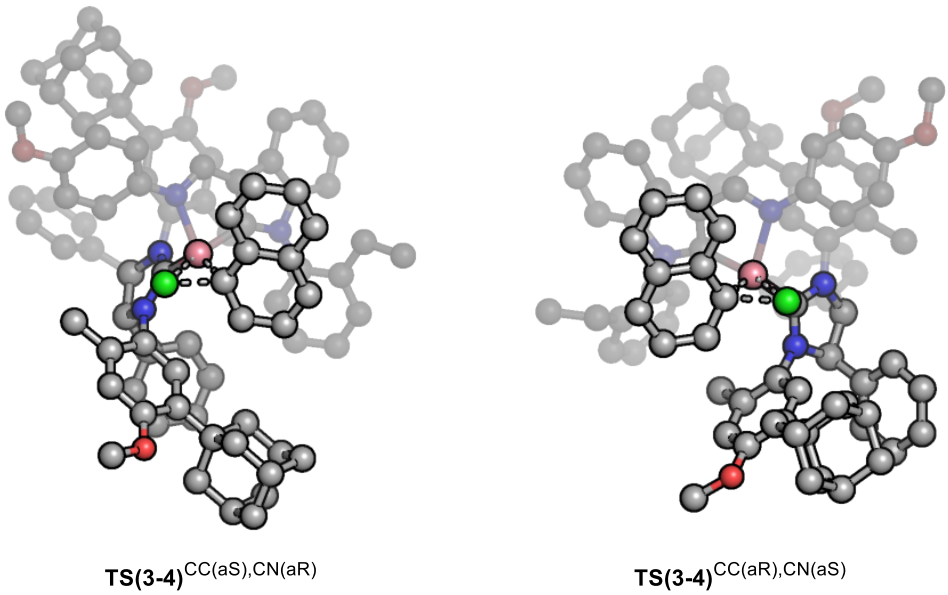

*Figure 4 : Optimized transition state structures for the oxidative addition elementary step in the triplet surface for the $aS_{C\text{-}N},aR_{C\text{-}C}$- and $aR_{C\text{-}N},aS_{C\text{-}C}$ -enantiomers obtained at theTPSS-D3(BJ)/def2-SVP level of theory with the chiral ligand **L*1**. Non-relevant hydrogens were omitted for clarity.*

Conclusions

In conclusion, we demonstrate herein that asymmetric C-H activation strategy opens new perspectives for the synthesis of complex, poly-chiral molecules. Unprecedented indole scaffolds featuringcinal HetAr-Ar and Ar-N atropisomeric axis could be prepared via Co-catalyzed enantioselective direct arylation. Excellent efficiencies, diastereoselectivities and

enantioselectivities were reached employing enantioure Co-NHC ligand, that promotes this challenging transformation under mild reaction conditions, thus warranting atropostability of the productd under reaction conditions. The mechanistic studies reveals origins of the diastereo- and enantio-selectivity of this transformation, that can be attributed to dispersive interactions during the oxidative addition step and the control of the C-N axial chirality within the metallation event.

---

[1] a) Ceramella, J., Iacopetta, D., Franchini, A., De Luca, M., Saturnino, C., Andreu, I., Sinicropi, M.S., and Catalano, A. (2022). A Look at the Importance of Chirality in Drug Activity: Some Significative Examples. Applied Sciences *12*, 10909. 10.3390/app122110909. b) Abram, M., Jakubiec, M., and Kamiński, K. (2019). Chirality as an Important Factor for the Development of New Antiepileptic Drugs. ChemMedChem *14*, 1744–1761. 10.1002/cmdc.201900367. c) Sekhon (2013). Exploiting the Power of Stereochemistry in Drugs: An Overview of Racemic and Enantiopure Drugs. J. Mod. Med. Chem. 10.12970/2308-8044.2013.01.01.2. d) Ananthi, N. (2018). Role of Chirality in Drugs. OMCIJ *5*. 10.19080/OMCIJ.2018.05.555661. e) Silvestri, I.P., and Colbon, P.J.J. (2021). The Growing Importance of Chirality in 3D Chemical Space Exploration and Modern Drug Discovery Approaches for Hit-ID: Topical Innovations. ACS Med. Chem. Lett. *12*, 1220–1229. 10.1021/acsmedchemlett.1c00251.

[2] Jeschke, P. (2018). Current status of chirality in agrochemicals: Chirality in agrochemicals. Pest. Manag. Sci. *74*, 2389–2404. 10.1002/ps.5052.

[3] a) Brandt, J.R., Salerno, F., and Fuchter, M.J. (2017). The added value of small-molecule chirality in technological applications. Nat Rev Chem *1*, 0045. 10.1038/s41570-017-0045. b) Wang, Y., Xiang, S., and Tan, B. (2021). Application in Drugs and Materials. In Axially Chiral Compounds, B. Tan, ed. (Wiley), pp. 297–315. 10.1002/9783527825172.ch11. c) Kuang, H., Xu, C., and Tang, Z. (2020). Emerging Chiral Materials. Adv. Mater. *32*, 2005110. 10.1002/adma.202005110. d) Zhao, B., Yang, S., Deng, J., and Pan, K. (2021). Chiral Graphene Hybrid Materials: Structures, Properties, and Chiral Applications. Adv. Sci. *8*, 2003681. 10.1002/advs.202003681.

[4] Bao, X., Rodriguez, J., and Bonne, D. (2020). Enantioselective Synthesis of Atropisomers with Multiple Stereogenic Axes. Angew. Chem. Int. Ed. *59*, 12623–12634. 10.1002/anie.202002518.

[5] a) Shibata, T., Tsuchikama, K., and Otsuka, M. (2006). Enantioselective intramolecular [2+2+2] cycloaddition of triynes for the synthesis of atropisomeric chiral ortho-diarylbenzene derivatives. Tetrahedron: Asymmetry *17*, 614–619. 10.1016/j.tetasy.2005.12.033.

[6] a) Wen, W., and Guo, Q. (2023). Atroposelective Construction of Triaryl *α* -Pyranones with 1,2-Diaxes by Asymmetric Organocatalysis. Chinese Journal of Organic Chemistry *43*, 781. 10.6023/cjoc202300007. b) Zhang, S., Wang, X., Han, L., Li, J., Liang, Z., Wei, D., and Du, D. (2022). Atroposelective Synthesis of Triaryl α-Pyranones with 1,2-Diaxes by N-Heterocyclic Carbene Organocatalysis. Angew Chem Int Ed *61*. 10.1002/anie.202212005. c) Zhang, S.-C., Liu, S., Wang, X., Wang, S.-J., Yang, H., Li, L., Yang, B., Wong, M.W., Zhao, Y., and Lu, S. (2023). Enantioselective Access to Triaryl-2-pyrones with Monoaxial or Contiguous C–C Diaxes via Oxidative NHC Catalysis. ACS Catal. *13*, 2565–2575. 10.1021/acscatal.2c05570.

[7] a) Wu, X., Witzig, R.M., Beaud, R., Fischer, C., Häussinger, D., and Sparr, C. (2021). Catalyst control over sixfold stereogenicity. Nat Catal *4*, 457–462. 10.1038/s41929-021-00615-z. b)

Lotter, D., Castrogiovanni, A., Neuburger, M., and Sparr, C. (2018). Catalyst-Controlled Stereodivergent Synthesis of Atropisomeric Multiaxis Systems. ACS Cent. Sci. *4*, 656–660. 10.1021/acscentsci.8b00204. c) Moser, D., and Sparr, C. (2022). Synthesis of Atropisomeric Two-Axis Systems by the Catalyst-Controlled *syn* - and *anti* -Selective Arene-Forming Aldol Condensation. Angew Chem Int Ed *61*. 10.1002/anie.202202548.

[8] Hu, Y.-L., Wang, Z., Yang, H., Chen, J., Wu, Z.-B., Lei, Y., and Zhou, L. (2019). Conversion of two stereocenters to one or two chiral axes: atroposelective synthesis of 2,3-diarylbenzoindoles. Chem. Sci. *10*, 6777–6784. 10.1039/C9SC00810A.

[9] a) Rodríguez-Salamanca, P., Fernández, R., Hornillos, V., and Lassaletta, J.M. (2022). Asymmetric Synthesis of Axially Chiral C−N Atropisomers. Chemistry A European J *28*. 10.1002/chem.202104442. b) Frey, J., Choppin, S., Colobert, F., and Wencel-Delord, J. (2020). Towards Atropoenantiopure N–C Axially Chiral Compounds *via* Stereoselective C–N Bond Formation. chimia (aarau) *74*, 883–889. 10.2533/chimia.2020.883. c) Kumarasamy, E., Raghunathan, R., Sibi, M.P., and Sivaguru, J. (2015). Nonbiaryl and Heterobiaryl Atropisomers: Molecular Templates with Promise for Atropselective Chemical Transformations. Chemical Reviews *115*, 11239–11300. 10.1021/acs.chemrev.5b00136. d) Wu, Y.-J., Liao, G., and Shi, B.-F. (2022). Stereoselective construction of atropisomers featuring a C–N chiral axis. Green Synthesis and Catalysis *3*, 117–136. 10.1016/j.gresc.2021.12.005.

[10] Oppenheimer, J., Hsung, R.P., Figueroa, R., and Johnson, W.L. (2007). Stereochemical Control of Both C−C and C−N Axial Chirality in the Synthesis of Chiral *N* , *O*- Biaryls. Org. Lett. *9*, 3969–3972. 10.1021/ol701692m.

[11] Xu, D., Huang, S., Hu, F., Peng, L., Jia, S., Mao, H., Gong, X., Li, F., Qin, W., and Yan, H. (2022). Diversity-Oriented Enantioselective Construction of Atropisomeric Heterobiaryls and *N* -Aryl Indoles via Vinylidene *Ortho* -Quinone Methides. CCS Chem *4*, 2686–2697. 10.31635/ccschem.021.202101154.

[12] Wang, B., Xu, G., Huang, Z., Wu, X., Hong, X., Yao, Q., and Shi, B. (2022). Single-Step Synthesis of Atropisomers with Vicinal C−C and C−N Diaxes by Cobalt-Catalyzed Atroposelective C−H Annulation. Angew Chem Int Ed *61*. 10.1002/anie.202208912.

[13] Gillooly, K.M., Pulicicchio, C., Pattoli, M.A., Cheng, L., Skala, S., Heimrich, E.M., McIntyre, K.W., Taylor, T.L., Kukral, D.W., Dudhgaonkar, S., et al. (2017). Bruton's tyrosine kinase inhibitor BMS-986142 in experimental models of rheumatoid arthritis enhances efficacy of agents representing clinical standard-of-care. PLoS ONE *12*, e0181782. 10.1371/journal.pone.0181782.

[14] Lanman, B.A., Parsons, A.T., and Zech, S.G. (2022). Addressing Atropisomerism in the Development of Sotorasib, a Covalent Inhibitor of KRAS G12C: Structural, Analytical, and Synthetic Considerations. Acc. Chem. Res. *55*, 2892–2903. 10.1021/acs.accounts.2c00479.

[15] Beutner, G., Carrasquillo, R., Geng, P., Hsiao, Y., Huang, E.C., Janey, J., Katipally, K., Kolotuchin, S., La Porte, T., Lee, A., et al. (2018). Adventures in Atropisomerism: Total Synthesis of a Complex Active Pharmaceutical Ingredient with Two Chirality Axes. Org. Lett. *20*, 3736–3740. 10.1021/acs.orglett.8b01218.

[16] For selected reviews see : a) Rogge, T., Kaplaneris, N., Chatani, N., Kim, J., Chang, S., Punji, B., Schafer, L.L., Musaev, D.G., Wencel-Delord, J., Roberts, C.A., et al. (2021). C–H activation. Nat Rev Methods Primers *1*, 43. 10.1038/s43586-021-00041-2. b) Dhawa, U., Kaplaneris, N., and Ackermann, L. (2021). Green strategies for transition metal-catalyzed C–H activation in molecular syntheses. Org. Chem. Front. *8*, 4886–4913. 10.1039/D1QO00727K. c) Sambiagio, C., Schönbauer, D., Blieck, R., Dao-Huy, T., Pototschnig, G., Schaaf, P., Wiesinger, T., Zia, M.F., Wencel-Delord, J., Besset, T., et al. (2018). A comprehensive overview of directing groups applied in metal-catalysed C–H functionalisation chemistry. Chemical Society Reviews *47*, 6603–6743. 10.1039/C8CS00201K. d) Zhang, L., and Ritter, T.

(2022). A Perspective on Late-Stage Aromatic C–H Bond Functionalization. J. Am. Chem. Soc. *144*, 2399–2414. 10.1021/jacs.1c10783. e) Dalton, T., Faber, T., and Glorius, F. (2021). C–H Activation: Toward Sustainability and Applications. ACS Cent. Sci., acscentsci.0c01413. 10.1021/acscentsci.0c01413.

[17] For selected reviews see : a) Carmona, J.A., Rodríguez-Franco, C., Fernández, R., Hornillos, V., and Lassaletta, J.M. (2021). Atroposelective transformation of axially chiral (hetero)biaryls. From desymmetrization to modern resolution strategies. Chem. Soc. Rev. *50*, 2968–2983. 10.1039/D0CS00870B. b) Colobert, F., and Wencel-Delord, J. (2019). C-H activation for asymmetric synthesis. c) Newton, C.G., Wang, S.-G., Oliveira, C.C., and Cramer, N. (2017). Catalytic Enantioselective Transformations Involving C–H Bond Cleavage by Transition-Metal Complexes. Chem. Rev. 10.1021/acs.chemrev.6b00692. d) Diesel, J., and Cramer, N. (2019). Generation of Heteroatom Stereocenters by Enantioselective C–H Functionalization. ACS Catal. *9*, 9164–9177. 10.1021/acscatal.9b03194. e) Wencel-Delord, J., and Colobert, F. (2013). Asymmetric C(sp2)-H Activation. Chem. Eur. J. *19*, 14010–14017. 10.1002/chem.201302576. f) Saint-Denis, T.G., Zhu, R.-Y., Chen, G., Wu, Q.-F., and Yu, J.-Q. (2018). Enantioselective C(sp ^{3})–H bond activation by chiral transition metal catalysts. Science *359*, eaao4798. 10.1126/science.aao4798.

[18] a) Jang, Y.-S., Woźniak, Ł., Pedroni, J., and Cramer, N. (2018). Access to *P* - and Axially Chiral Biaryl Phosphine Oxides by Enantioselective Cp ^{x} Ir ^{III} -Catalyzed C−H Arylations. Angew. Chem. Int. Ed. *57*, 12901–12905. 10.1002/anie.201807749. b) Romero-Arenas, A., Hornillos, V., Iglesias-Sigüenza, J., Fernández, R., López-Serrano, J., Ros, A., and Lassaletta, J.M. (2020). Ir-Catalyzed Atroposelective Desymmetrization of Heterobiaryls: Hydroarylation of Vinyl Ethers and Bicycloalkenes. J. Am. Chem. Soc. *142*, 2628–2639. 10.1021/jacs.9b12858. c) Wang, F., Jing, J., Zhao, Y., Zhu, X., Zhang, X., Zhao, L., Hu, P., Deng, W., and Li, X. (2021). Rhodium-Catalyzed C−H Activation-Based Construction of Axially and Centrally Chiral Indenes through Two Discrete Insertions. Angew. Chem. Int. Ed. *60*, 16628–16633. 10.1002/anie.202105093. d) Li, Y., Liou, Y., Oliveira, J.C.A., and Ackermann, L. (2022). Ruthenium(II)/Imidazolidine Carboxylic Acid-Catalyzed C−H Alkylation for Central and Axial Double Enantio-Induction. Angew Chem Int Ed *61*. 10.1002/anie.202212595. e) Hu, P., Kong, L., Wang, F., Zhu, X., and Li, X. (2021). Twofold C−H Activation-Based Enantio- and Diastereoselective C−H Arylation Using Diarylacetylenes as Rare Arylating Reagents. Angew Chem Int Ed *60*, 20424–20429. 10.1002/anie.202106871. f) Wang, J., Chen, H., Kong, L., Wang, F., Lan, Y., and Li, X. (2021). Enantioselective and Diastereoselective C–H Alkylation of Benzamides: Synergized Axial and Central Chirality via a Single Stereodetermining Step. ACS Catal. *11*, 9151–9158. 10.1021/acscatal.1c02450.

[19] a) Gao, Q., Wu, C., Deng, S., Li, L., Liu, Z.-S., Hua, Y., Ye, J., Liu, C., Cheng, H.-G., Cong, H., et al. (2021). Catalytic Synthesis of Atropisomeric *o* -Terphenyls with 1,2-Diaxes via Axial-to-Axial Diastereoinduction. J. Am. Chem. Soc. *143*, 7253–7260. 10.1021/jacs.1c02405. b) Dherbassy, Q., Djukic, J.-P., Wencel-Delord, J., and Colobert, F. (2018). Two Stereoinduction Events in One C−H Activation Step: A Route towards Terphenyl Ligands with Two Atropisomeric Axes. Angewandte Chemie International Edition *57*, 4668–4672. 10.1002/anie.201801130.

[20] a) Punji, B., Song, W., Shevchenko, G.A., and Ackermann, L. (2013). Cobalt-Catalyzed C-H Bond Functionalizations with Aryl and Alkyl Chlorides. Chem. Eur. J. *19*, 10605–10610. 10.1002/chem.201301409. b) Gao, K., Lee, P.-S., Long, C., and Yoshikai, N. (2012). Cobalt-Catalyzed *Ortho* -Arylation of Aromatic Imines with Aryl Chlorides. Org. Lett. *14*, 4234–4237. 10.1021/ol301934y. c) Song, W., and Ackermann, L. (2012). Cobalt-Catalyzed Direct Arylation and Benzylation by C-H/C-O Cleavage with Sulfamates, Carbamates, and Phosphates. Angew. Chem. Int. Ed. *51*, 8251–8254. 10.1002/anie.201202466.

[21] a) Loup, J., Dhawa, U., Pesciaioli, F., Wencel-Delord, J., and Ackermann, L. (2019). Enantioselective C−H Activation with Earth-Abundant 3d Transition Metals. Angew. Chem. Int. Ed. *58*, 12803–12818. 10.1002/anie.201904214. b) Woźniak, Ł., and Cramer, N. (2019). Enantioselective C H Bond Functionalizations by 3d Transition-Metal Catalysts. Trends in Chemistry *1*, 471–484. 10.1016/j.trechm.2019.03.013.

[22] a) Jacob, N., Zaid, Y., Oliveira, J.C.A., Ackermann, L., and Wencel-Delord, J. (2022). Cobalt-Catalyzed Enantioselective C–H Arylation of Indoles. J. Am. Chem. Soc. *144*, 798–806. 10.1021/jacs.1c09889. b) Song, W., and Ackermann, L. (2012). Cobalt-Catalyzed Direct Arylation and Benzylation by C-H/C-O Cleavage with Sulfamates, Carbamates, and Phosphates. Angew. Chem. Int. Ed. *51*, 8251–8254. 10.1002/anie.201202466.

[23] Loup, J., Zell, D., Oliveira, J.C.A., Keil, H., Stalke, D., and Ackermann, L. (2017). Asymmetric Iron-Catalyzed C−H Alkylation Enabled by Remote Ligand *meta* -Substitution. Angew. Chem. Int. Ed. *56*, 14197–14201. 10.1002/anie.201709075.

[24] Cristallographic data are available free of charge on CCDC number: CDC: 2253011

[25] Chen, S., Feng, B., Zheng, X., Yin, J., Yang, S., and You, J. (2017). Iridium-Catalyzed Direct Regioselective C4-Amidation of Indoles under Mild Conditions. Org. Lett. *19*, 2502–2505. 10.1021/acs.orglett.7b00730.

[26] Kalepu, J., Gandeepan, P., Ackermann, L., and Pilarski, L.T. (2018). C4–H indole functionalisation: precedent and prospects. Chem. Sci. *9*, 4203–4216. 10.1039/C7SC05336C.